ARTICLES
PUBLISHED ONLINE: 25 APRIL 2016 | DOI: 10.1038/NMAT4629
nature materials

Promoting solution phase discharge in Li–O_2 batteries containing weakly solvating electrolyte solutions

Xiangwen Gao†, Yuhui Chen†, Lee Johnson and Peter G. Bruce*

On discharge, the Li–O_2 battery can form a Li_2O_2 film on the cathode surface, leading to low capacities, low rates and early cell death, or it can form Li_2O_2 particles in solution, leading to high capacities at relatively high rates and avoiding early cell death. Achieving discharge in solution is important and may be encouraged by the use of high donor or acceptor number solvents or salts that dissolve the LiO_2 intermediate involved in the formation of Li_2O_2. However, the characteristics that make high donor or acceptor number solvents good (for example, high polarity) result in them being unstable towards LiO_2 or Li_2O_2. Here we demonstrate that introduction of the additive 2,5-di-*tert*-butyl-1,4-benzoquinone (DBBQ) promotes solution phase formation of Li_2O_2 in low-polarity and weakly solvating electrolyte solutions. Importantly, it does so while simultaneously suppressing direct reduction to Li_2O_2 on the cathode surface, which would otherwise lead to Li_2O_2 film growth and premature cell death. It also halves the overpotential during discharge, increases the capacity 80- to 100-fold and enables rates $>1\,mA\,cm^{-2}_{areal}$ for cathodes with capacities of $>4\,mAh\,cm^{-2}_{areal}$. The DBBQ additive operates by a new mechanism that avoids the reactive LiO_2 intermediate in solution.

The high theoretical specific energy of the rechargeable Li–O_2 battery has generated intense interest in the possibility of a practical device that could deliver energy storage significantly in excess of today's lithium-ion batteries[1–9]. However, major challenges hinder the development of such a technology[1–6,10–14]. Typically a Li–O_2 battery is composed of a lithium metal anode separated by an aprotic electrolyte solution from a porous O_2 cathode. The reaction at the cathode involves, on discharge, the reduction of O_2 to form Li_2O_2, with oxidation of the latter on charge. Growth of Li_2O_2 on the cathode surface leads to low capacities, poor rates and early cell death[15–17]. In contrast, if Li_2O_2 can be induced to grow in the electrolyte solution then high discharge capacities at relatively high rates and avoiding early cell death is possible[15]. It is clearly important to operate a Li–O_2 battery in which Li_2O_2 grows in solution.

A number of groups have elucidated the mechanism of O_2 reduction to Li_2O_2 on discharge[15,16,18–21]. The reduction proceeds through the following general steps:

$$O_2 + Li^+ + e^- \rightarrow LiO_2 \quad (1)$$

$$2LiO_2 \rightarrow Li_2O_2 + O_2 \quad (2)$$

$$LiO_2 + Li^+ + e^- \rightarrow Li_2O_2 \quad (3)$$

Whether Li_2O_2 grows in solution or as a film on the electrode surface depends on the solubility of the LiO_2 intermediate; if LiO_2 dissolves in the electrolyte solution then Li_2O_2 grows in solution. Solubility of LiO_2 depends on the strength of the cation and anion solvation, that is, on the solvent and salt donor and acceptor numbers[15,22–24]. However, the properties that make a good solvent for LiO_2 (for example, high polarity) often make the solvent more susceptible to nucleophilic attack or proton abstraction by the reactive O_2^- radical, leading to undesirable side reactions. The challenge is to form Li_2O_2 in solution on discharge in low donor number (weakly solvating) solvents.

Soluble catalysts or salts with high donor numbers can in principle promote solution phase growth of Li_2O_2 in low donor number solvents (for example, ethers)[22,27–30]. High donor number salts have been shown to increase the capacity fourfold and reduce the discharge overpotential by ~30–50 mV over low donor number salts[22]. Viologens[27,28], phthalocyanines[29] and quinones[30] have been investigated as possible soluble reduction catalysts. Although the studies of such catalysts are important, in most cases there is little or no direct evidence demonstrating that they promote formation of Li_2O_2 in solution and not on the electrode surface because they rely on electrochemical measurements alone. Yet past work on Li–O_2 batteries has shown how essential it is to provide more than electrochemical evidence in this field[31]. In some cases, soluble catalysts show an increase in discharge voltage (lower overpotential) as small as, for example, 40 mV (refs 28,29), which is very unlikely to be sufficient to shut off the direct reduction of O_2 to Li_2O_2, essential to stop detrimental Li_2O_2 film formation. Also, none of the previous studies in low donor number solvents exhibited a significant increase in capacity on discharge at a relatively high rate, which is important for a successful Li–O_2 battery.

Here we demonstrate that addition of DBBQ (2,5-di-*tert*-butyl-1,4-benzoquinone) to a weakly solvating (low donor number) electrolyte solution, LiTFSI in ether[22], promotes O_2 reduction to Li_2O_2 in solution while halving the discharge overpotential (increasing the discharge potential), suppressing the growth of a Li_2O_2 film on the electrode surface, thus postponing cell death, increasing the discharge capacity 80–100-fold and permitting discharge at relatively

Departments of Materials and Chemistry, Parks Road, University of Oxford, Oxford OX1 3PH, UK. †These authors contributed equally to this work.
*e-mail: peter.bruce@materials.ox.ac.uk

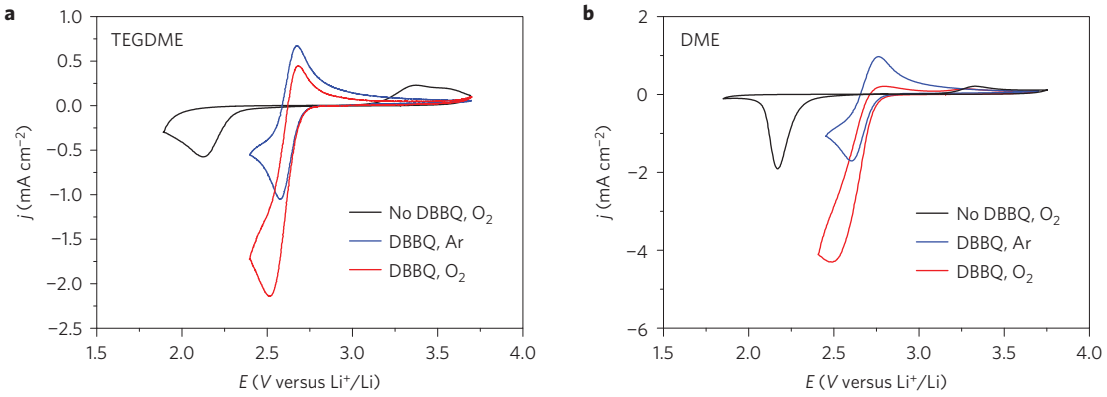

Figure 1 | Cyclic voltammograms demonstrating the significant effect that DBBQ has on O_2 reduction in ethers. a,**b**, Cyclic voltammograms for DBBQ in 1 M LiTFSI in TEGDME (**a**) and DME (**b**). Cyclic voltammograms under Ar (blue) and O_2 (red) and for direct O_2 reduction without DBBQ (black). DBBQ concentration was 10 mM and cyclic voltammograms were carried out at planar Au electrodes; scan rate 100 mV s^{-1}.

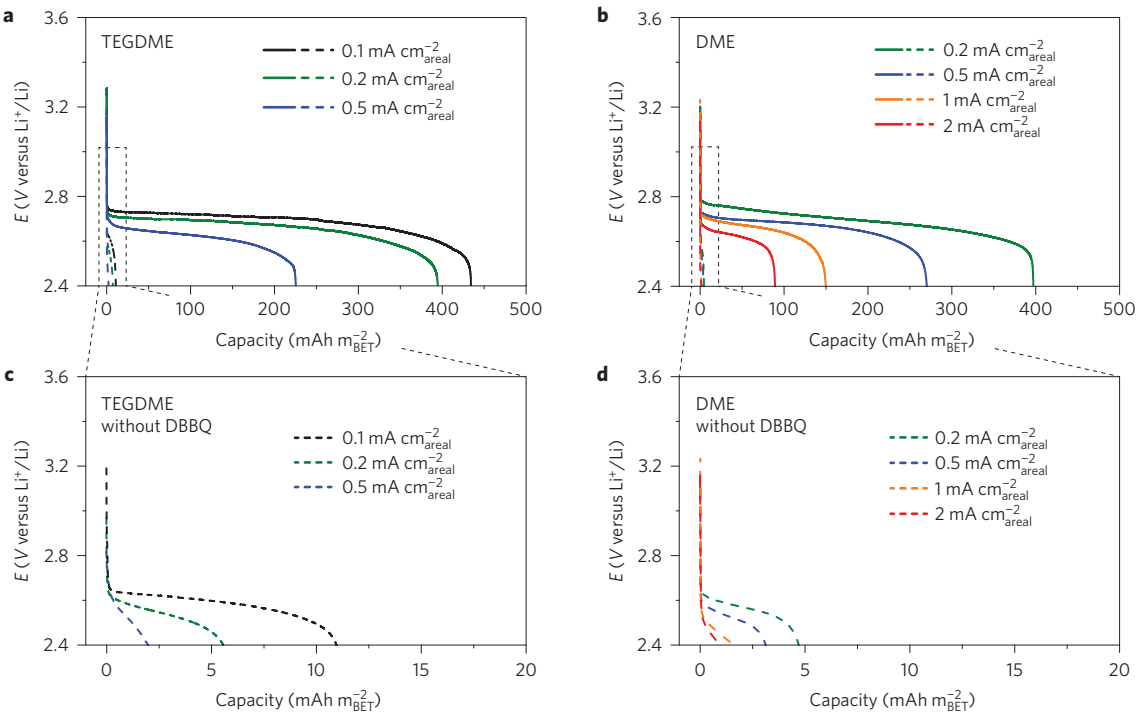

Figure 2 | Significant effect of DBBQ on discharge in ethers. a,**b**, Load curves of oxygen reduction at a gas diffusion electrode discharged in 1 M LiTFSI in TEGDME (**a**) and DME (**b**) with 10 mM DBBQ (solid lines) and without DBBQ (dashed lines) under O_2 at various areal current densities from 0.1 mA cm^{-2} to 2 mA cm^{-2}. **c**,**d**, Enlarged section of the load curves recorded without DBBQ in **a**,**b**. Two hundred microlitres of electrolyte was used. The roughness factor of the cathode is 270. The amounts of Li_2O_2 formed on discharge were 10.0, 9.1 and 5.2 mg cm^{-2}_{areal} in TEDGME, and 9.1, 6.3, 3.4 and 2.0 mg cm^{-2}_{areal} in DME.

high rates >1 mA cm^{-2}_{areal} for an electrode capacity of >4 mAh cm^{-2}_{areal}. It operates by a new mechanism that does not involve the reactive LiO_2 as an intermediate; the new mechanism also decouples the link between the nature of the electrolyte solution (solvating power) and the nature of the product (particles or surface film). The search for truly stable electrolyte solutions for Li–O_2 batteries will focus on very low-polarity and hence weakly solvating solvents. The significance of the present work is that if such stable solvents can be identified then DBBQ provides a route to solution growth of Li_2O_2 and hence potentially high rates, high capacities and sustained cycling, avoiding early cell death.

Cyclic voltammetry studies with DBBQ

The potential at which O_2 is reduced to Li_2O_2 (the discharge plateau in a Li–O_2 cell) is lower than the thermodynamic potential for O_2/Li_2O_2, 2.96 V. A cyclic voltammogram corresponding to this process is shown in Fig. 1. To promote O_2 reduction to Li_2O_2 in solution in low donor number solvents while suppressing the direct reduction of O_2 to form a Li_2O_2 film, which would otherwise passivate the electrode[15,16,21], it is necessary to carry out the reduction of O_2 to Li_2O_2 in solution at a higher potential than the surface reaction, which also has the advantage of increasing the cell discharge potential closer to its thermodynamic potential of 2.96 V (reducing the overpotential). To achieve this, molecules with a redox potential higher than the potential at which O_2 is reduced (discharge plateau in a Li–O_2 cell) are required. Quinones were selected as they are known to exhibit potentials in the relevant range[30,32]. Several quinones were investigated but most were found not to enhance O_2 reduction (see Supplementary Fig. 1). Electrolyte preparation and cell assembly are described in the

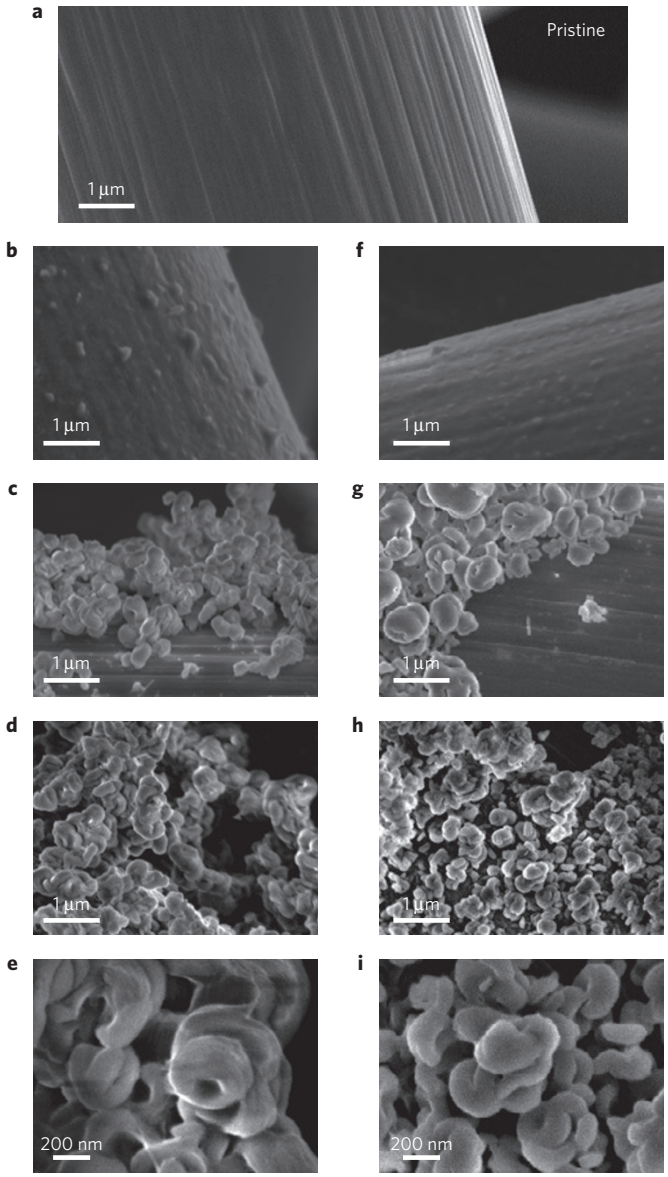

Figure 3 | SEM images showing the Li_2O_2 morphologies on discharge in 1 M LiTFSI in ethers with and without DBBQ. a, The pristine GDL. **b**–**i**, Discharge in TEGDME (**b**–**e**) and in DME (**f**–**i**). **b**,**f**, Full discharge without DBBQ. **c**,**g**, Half discharge with 10 mM DBBQ. **d**,**e**,**h**,**i**, Full discharge with DBBQ.

Supplementary Information. DBBQ, in contrast, showed promising electrochemistry (Fig. 1). The cyclic voltammograms for DBBQ obtained in 1 M LiTFSI in tetraethylene glycol dimethyl ether (TEGDME) and dimethoxyethane (DME) at a gold electrode under Ar exhibit quasi-reversible behaviour (Fig. 1 and Supplementary Fig. 2). In the presence of O_2, the reduction peak is enhanced significantly. Such a cyclic voltammogram is similar to that of a catalysed reduction[33], where a redox-active species, in this case DBBQ, is reduced and then takes part in a chemical reaction, here with O_2 to form Li_2O_2, resulting in the rapid regeneration of more DBBQ, giving rise to the increased reduction current. The reduction potential is significantly higher than for the direct reduction of O_2 (Fig. 1), thus effectively suppressing the direct reduction of O_2 to Li_2O_2 films on the electrode surface. The mechanism of O_2 reduction by DBBQ is discussed further later; demonstration of the efficiency of DBBQ in promoting Li_2O_2 formation in solution and not on the electrode surface, as well as increasing the discharge potential of Li–O_2 cells is presented below.

Enhancing the discharge of Li–O_2 cells with DBBQ

Li–O_2 cells were constructed as described in the Supplementary Information (Methods). The cathode was a binder-free carbon-fibre gas diffusion layer (GDL, Freudenberg), similar to cathodes used widely for aprotic O_2 cells[20,34]. Carbon electrodes are relatively stable on discharge[35], which is our focus here. The anode consisted of Li_xFePO_4, as used in previous Li–O_2 studies instead of Li metal to avoid any oxidation of the anode by O_2 (ref. 36). The Li_xFePO_4 potential versus Li^+/Li, 3.45 V, was used to express all potentials in this work on the Li scale. The electrolyte solution was in all cases 1 M LiTFSI dissolved in the low donor and acceptor number ethers, TEGDME or DME.

Cells containing TEGDME and DME saturated with O_2 (under 1 atm of O_2) were each discharged at several different areal current densities with and without DBBQ (Fig. 2). In the absence of DBBQ, the cells died rapidly, exhibiting very small capacities and poor rate capability, in accord with previous observations[3,37]. The cells with DBBQ discharged under the same conditions exhibited a marked improvement, delivering up to ~80–100 times higher discharge capacities before end of life. In TEGDME with DBBQ, a capacity of 10.6 mAh cm^{-2}_{areal} (equivalent to 9.1 mg of Li_2O_2) was obtained at a current density of 0.2 mA cm^{-2}_{areal}, whereas in DME with DBBQ, 7.3 mAh cm^{-2}_{areal} (equivalent to 6.3 mg of Li_2O_2) was obtained at 0.5 mA cm^{-2}_{areal} and 4 mAh cm^{-2}_{areal} (equivalent to 3.4 mg of Li_2O_2) at 1 mA cm^{-2}_{areal}. Moreover, areal current densities of 0.5 mA cm^{-2} (in TEGDME) and 2 mA cm^{-2} (in DME) were achieved, while halving the discharge overpotential, compared with the performance in the absence of DBBQ. To estimate the contribution of DBBQ reduction itself to the capacity, the cells were discharged under Ar, for DME and TEGDME, and at the same current densities as in Fig. 2. The discharge curves are given in Supplementary Fig. 3. A negligible capacity was observed. These values are all within the limits of the theoretical capacity for DBBQ reduction of 12.5 mAh m^{-2}_{BET}.

It has been shown that the limit of Li_2O_2 film growth is ~6 nm (ref. 17), which equates to a maximum capacity of ~15 mAh m^{-2}_{BET} (0.4 mAh cm^{-2}_{areal}). As is evident in Fig. 2, the cells without DBBQ exhibit end of life below this limit, indicating that Li_2O_2 formation is predominantly by the surface route. In contrast, cells containing DBBQ are able to exceed the limit of film growth by an order of magnitude, signalling predominantly solution growth of Li_2O_2.

To confirm that Li_2O_2 grows primarily in solution, away from the electrode surface, in the presence of DBBQ, despite the use of low donor/acceptor solvents, the discharged cathodes with and without DBBQ were extracted and examined by scanning electron microscopy (SEM). The results are shown in Fig. 3. In both TEGDME and DME, in the absence of DBBQ, the surfaces of the carbon fibres that constitute the GDL were covered with a film and there was no evidence of Li_2O_2 particles. In contrast, identical cells discharged under the same conditions, except for the presence of DBBQ, show substantial growth of particles in the pores of the electrodes and with the toroidal morphologies expected for Li_2O_2 (Fig. 3). Equally important is that DBBQ suppresses film growth on the electrode surface. This is shown in Fig. 3c,g where there is little evidence of film growth when DBBQ was present until close to cell death. There will always be some direct reduction to form Li_2O_2 on the surface, even at the higher potential where DBBQ is reduced, as the direct reduction to form a Li_2O_2 film is suppressed but not eliminated completely. It has been proposed recently that the presence of H_2O can itself promote Li_2O_2 toroid formation in Li–O_2 batteries[16,20]. Care was taken to rigorously dry the solvents, electrodes and all cell components used here. The H_2O content at the beginning and end of discharge did not exceed 30 ppm, considerably smaller than the quantities required to promote toroid formation; at least 200~500 ppm H_2O is needed[16,20]. Overall, the SEM images demonstrate that DBBQ has successfully displaced the O_2 reduction away from the electrode surface, promoting growth

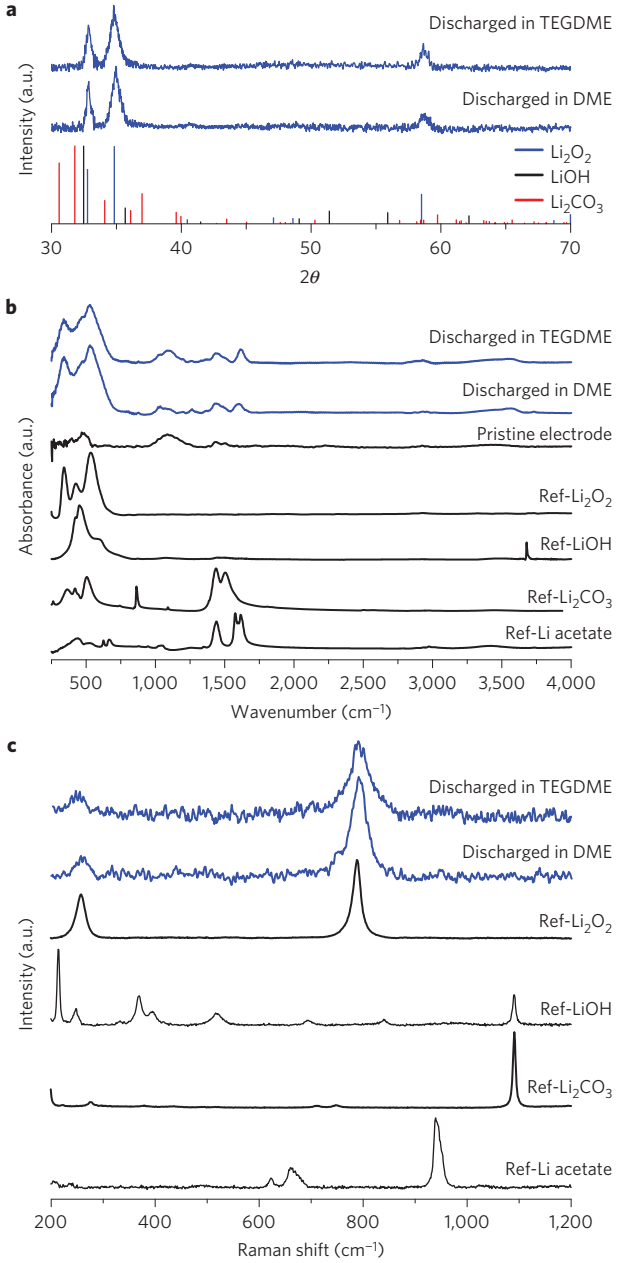

Figure 4 | Characterization of the discharge product confirming that Li_2O_2 is dominant. a–c, PXRD pattern (**a**), infrared (**b**) and Raman spectra (**c**) of GDLs discharged in 10 mM DBBQ–1 M LiTFSI in TEGDME and DME under O_2.

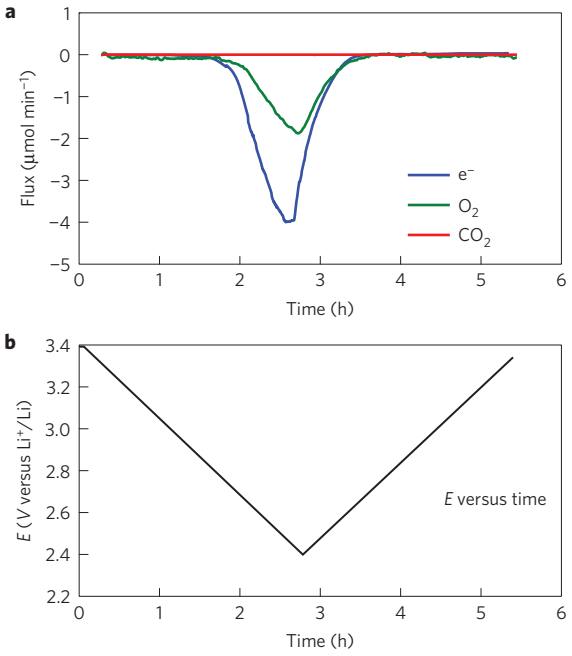

Figure 5 | *In situ* DEMS in DBBQ–TEGDME showing 2.03 e^- per O_2 consumed, consistent with formation of Li_2O_2. a, Discharge current (blue), O_2 consumption (green) and CO_2 evolution (red) in 10 mM DBBQ–1 M LiTFSI in TEGDME. **b**, Voltage profile of the DEMS cell. Cyclic voltammetry was applied. The e^-/O_2 ratio was obtained from the integral of charge passed and total O_2 consumption.

of large Li_2O_2 particles in the adjacent solution within the pores of the electrode.

To demonstrate that the particles observed in SEM are indeed Li_2O_2, powder X-ray diffraction (PXRD), infrared spectrometry and Raman spectroscopy were carried out on the porous electrodes extracted from the cells. The results are presented in Fig. 4. The PXRD pattern collected on the GDLs discharged in ethers exhibits only peaks associated with Li_2O_2. The results are confirmed by the infrared and Raman spectra in Fig. 4, which also show Li_2O_2 as the primary product. Although ethers are one of the more stable solvents in Li–O_2 batteries, it is known that they are not completely stable[38]. Small peaks associated with lithium acetate/formate and some Li_2CO_3 are evident as minor by-products in the infrared spectra, as identified previously for discharge in ethers[39]. There is little evidence of LiOH. To investigate the presence of any soluble by-products, NMR was carried out on the electrolyte solutions. The details are described in the Methods. In addition to the peaks associated with the electrolyte solutions, only a tiny peak assigned to lithium acetate was observed (Supplementary Fig. 4). *In situ* differential electrochemical mass spectrometry (DEMS) was carried out to investigate the gas consumption on discharge. The procedure is described in the Supplementary Information and the results are presented in Fig. 5. No gases were detected other than O_2 and in particular there was no evidence of CO_2, consistent with the degree of side reactions in ethers being small. The total O_2 consumed and total charge passed were measured and the integral gave a ratio of electrons to oxygen consumed of 2.03 e^-/O_2, consistent with the dominant reaction on discharge involving Li_2O_2 formation[38,40]. These results are in accord with charge/mass ratios seen previously for ethers[38]. Taken together, the PXRD, infrared, Raman and DEMS results indicate that the dominant product on discharge in the presence of DBBQ in ethers is Li_2O_2 and that it forms relatively large particles in the pores rather than on the surfaces of the porous electrode. The amount of Li_2O_2 present in the electrode was quantified by chemical analysis using $TiOSO_4$ as described in the Supplementary Information. The yield of Li_2O_2 (observed mass/mass predicted from charge passed) with DBBQ was 95% and 86% in DME and TEGDME, respectively. This compares with 91% and 81% reported previously for DME and TEGDME in the absence of DBBQ[38]. The slightly higher yields indicate that the relatively high surface area of the Li_2O_2 film that grows on the electrode in the absence of DBBQ leads to more decomposition of the electrolyte solution than is the case for the large particles in solution. It has also been suggested that LiO_2 is responsible for solvent decomposition on discharge[26,41,42] and, as discussed below, our analysis points to a mechanism that avoids this reactive intermediate.

Attempts to charge the cells after discharge proved fruitless (see Supplementary Fig. 5). This is to be expected because the Li_2O_2 is not well connected to the electrode surface and therefore direct electrochemical oxidation will be difficult. Therefore, especially in

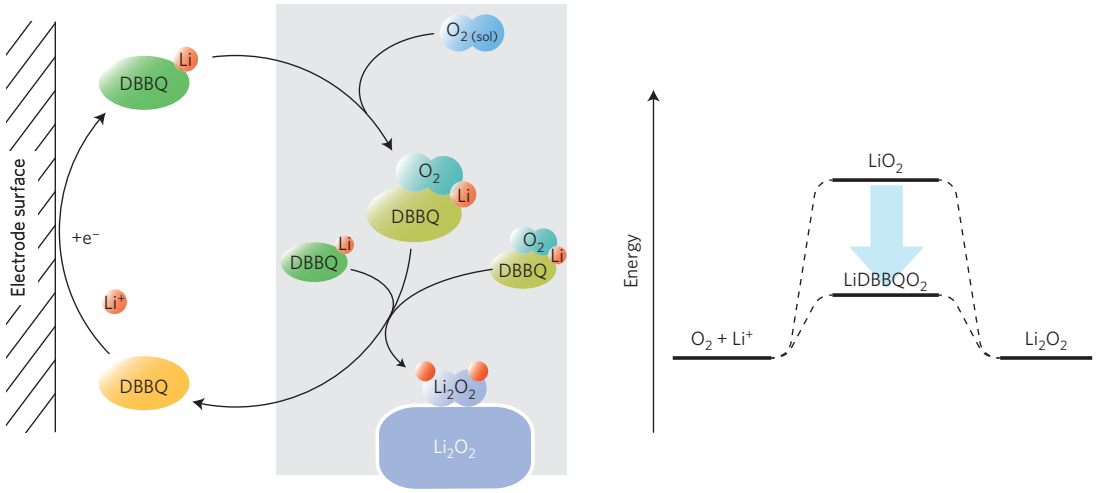

Figure 6 | Schematics of reactions on discharge (left) and the effect of DBBQ on the potential determining step (right). DBBQ is reduced at the electrode surface, forming LiDBBQ, and then LiDBBQ reacts with O_2, producing Li_2O_2 and itself being regenerated to DBBQ. The schematic of the free-energy plot is at E^0 for O_2/Li_2O_2.

the presence of a reduction-mediated discharge, it will be necessary to employ an oxidation mediator to charge the cell, as described previously[36,43–45].

The mechanism of O_2 reduction in the presence of DBBQ

As mentioned above, DBBQ does not operate as an electrocatalyst like, for example, the phthalocyanines described previously[29,46], for which O_2 is bound to the electrocatalyst before, during and after reduction. Neither does it operate as a redox shuttle, transferring electrons from the electrode surface to reduce O_2 in solution to LiO_2 and further to Li_2O_2 by an outer-sphere reaction. Instead, it operates by a different mechanism that changes the pathway of O_2 reduction to Li_2O_2 avoiding the reactive LiO_2 as an intermediate.

The reduction of quinones, such as DBBQ, in Li^+ electrolyte solutions under Ar is known to form Li–quinone complexes, in this case LiDBBQ (Fig. 1)[47–49]. In the presence of O_2, the reduction potential for DBBQ/LiDBBQ does not change (Fig. 1), indicating that the same reduction reaction (DBBQ to LiDBBQ) occurs. Therefore, there is no binding of O_2 to DBBQ before the initial electron transfer, unlike the phthalocyanines[29]; the first step is as shown in equation (4). However, the reduction current is enhanced significantly (Fig. 1). The observed cyclic voltammogram is similar to that of an EC_{cat} reaction, electrochemical reduction followed by a chemical step, in which the reduced form of the redox couple takes part in a chemical reaction that regenerates the oxidized form of the couple to feed the reduction[33]. Here, DBBQ is regenerated from LiDBBQ by the latter reducing O_2 in a chemical step, which goes on to form Li_2O_2.

In the absence of DBBQ, reduction of O_2 to Li_2O_2 proceeds via the LiO_2 intermediate[15,16,18–21], and it is the need to reach the potential for formation of LiO_2 that pins the O_2 reduction at a potential (discharge plateau in a Li–O_2 cell) significantly negative of the standard potential for Li_2O_2 formation, 2.96 V (Fig. 1). Where the energetics of an intermediate dictates the potential required to carry out an electrochemical reaction, this is referred to as a 'thermodynamic overpotential'[50]. In the presence of DBBQ, O_2 reduction effectively takes place at the potential for DBBQ reduction (Fig. 1), that is, at a significantly higher potential than would be the case if O_2 reduction was occurring via the LiO_2 intermediate in solution. This indicates that O_2 reduction does not follow the usual path via the LiO_2 intermediate but involves formation of a different intermediate complex between LiDBBQ and O_2. By complexing Li^+ and O_2 with $DBBQ^-$, the reaction path and hence free energy of the intermediate (now a complex of the form $LiDBBQO_2$ not LiO_2) is lowered (Fig. 6) and the potential correspondingly raised, as seen in the higher voltage for the discharge plateau in galvanostatic discharge of Li–O_2 cells (Fig. 2).

The sequence of proposed reaction steps at the cathode on discharging a Li–O_2 cell containing DBBQ is summarized in equations (4)–(6). Equation (4) is the initial electrochemical reduction. Equations (6) and (7) are examples of possible steps by which the intermediate formed in (5) could disproportionate or react with another LiDBBQ, to form Li_2O_2 that grows from solution, as observed in, for example, Fig. 3. Confirmation that LiDBBQ and O_2 react together to form Li_2O_2 was obtained by a direct chemical experiment in which O_2 was bubbled through a solution containing LiDBBQ and the quantity of Li_2O_2 measured by $TiOSO_4$ titration (see Supplementary Information for details).

$$DBBQ_{(sol)} + Li^+_{(sol)} + e^- \rightarrow LiDBBQ_{(sol)} \quad (4)$$

$$LiDBBQ_{(sol)} + O_{2(sol)} \rightleftharpoons LiDBBQO_{2(sol)} \quad (5)$$

$$2LiDBBQO_{2(sol)} \rightarrow Li_2O_{2(s)} + O_{2(sol)} + 2DBBQ_{(sol)} \quad (6)$$

$$LiDBBQ_{(sol)} + LiDBBQO_{2(sol)} \rightarrow Li_2O_{2(s)} + 2DBBQ_{(sol)} \quad (7)$$

These reactions can be summarized by the schematic shown in Fig. 6, and the consequences of this scheme are relatively simple electron transfer and dominate solution phase product formation that translate into high rates and capacities during cell discharge.

As noted above, DBBQ does not act as a conventional catalyst, it does not bind O_2 and facilitate LiO_2 formation by stabilizing the superoxide intermediate. Instead DBBQ is reduced to LiDBBQ that binds O_2 to form $LiDBBQO_2$ (equation (5)). The characteristics that make DBBQ suitable for this function are: a reduction potential positive of the potential for formation of LiO_2 formation, thus avoiding direct formation of LiO_2; a reduction potential negative of the overall reduction potential to Li_2O_2 such that a driving force remains to push the reaction towards peroxide formation; and the ability to bind O_2 when in the reduced form (LiDBBQ).

Outlook

O_2 reduction to Li_2O_2 by the DBBQ-mediated route brings a number of benefits. The electrochemistry at the electrode surface is now

DBBQ reduction rather than direct formation of Li_2O_2, in an electrolyte solution that does not dissolve LiO_2 (weakly solvating electrolyte solution). As a result, Li_2O_2 formation is moved into solution without the need for high donor/acceptor number solvents or salts. DBBQ shuts down the direct formation of a Li_2O_2 film on the cathode, which postpones cell death, increases capacity 80–100-fold, and facilitates discharge rates of $>1\,mA\,cm^{-2}_{areal}$ for cathodes with capacities of $>4\,mAh\,cm^{-2}_{areal}$. The discharge potential is also increased (overpotential is halved). O_2 reduction to Li_2O_2 in the presence of DBBQ follows a new route that avoids the reactive LiO_2 in solution. The search for truly stable electrolyte solutions for Li–O_2 batteries will focus on very low-polarity and hence weakly solvating solvents. The significance of the present work is that if such stable solvents can be identified then DBBQ provides a route to solution growth of Li_2O_2 and hence potentially high rates, high capacities and sustained cycling, avoiding early cell death. These results demonstrate the importance of moving to a mediated reaction on reduction and imply that the future of the lithium–air battery involves the mediated formation and decomposition of lithium peroxide, where the latter only fulfils the role of storage medium.

Methods

Methods and any associated references are available in the online version of the paper.

Received 18 November 2015; accepted 21 March 2016; published online 25 April 2016; corrected online 16 June 2016

References

1. Abraham, K. M. & Jiang, Z. A polymer electrolyte-based rechargeable lithium/oxygen battery. *J. Electrochem. Soc.* **143,** 1–5 (1996).
2. Bruce, P. G., Freunberger, S. A., Hardwick, L. J. & Tarascon, J.-M. Li–O_2 and Li–S batteries with high energy storage. *Nature Mater.* **11,** 19–29 (2012).
3. Girishkumar, G., McCloskey, B., Luntz, A. C., Swanson, S. & Wilcke, W. Lithium-air battery: promise and challenges. *J. Phys. Chem. Lett.* **1,** 2193–2203 (2010).
4. Shao, Y. *et al*. Electrocatalysts for nonaqueous lithium-air batteries: status, challenges, and perspective. *ACS Catal.* **2,** 844–857 (2012).
5. Christensen, J. *et al*. A critical review of Li/air batteries. *J. Electrochem. Soc.* **159,** R1–R30 (2012).
6. Black, R., Adams, B. & Nazar, L. F. Non-aqueous and hybrid Li–O_2 batteries. *Adv. Energy Mater.* **2,** 801–815 (2012).
7. Choi, N. S. *et al*. Challenges facing lithium batteries and electrical double-layer capacitors. *Angew. Chem. Int. Ed.* **51,** 9994–10024 (2012).
8. Etacheri, V., Marom, R., Elazari, R., Salitra, G. & Aurbach, D. Challenges in the development of advanced Li–ion batteries: a review. *Energy Environ. Sci.* **4,** 3243–3262 (2011).
9. Zhang, T. *et al*. A novel high energy density rechargeable lithium/air battery. *Chem. Commun.* **46,** 1661–1663 (2010).
10. Luntz, A. C. & McCloskey, B. D. Nonaqueous Li–air batteries: a status report. *Chem. Rev.* **114,** 11721–11750 (2014).
11. Li, F., Zhang, T. & Zhou, H. Challenges of non-aqueous Li–O_2 batteries: electrolytes, catalysts, and anodes. *Energy Environ. Sci.* **6,** 1125–1141 (2013).
12. Thackeray, M. M., Chan, M. K. Y., Trahey, L., Kirklin, S. & Wolverton, C. Vision for designing high-energy, hybrid Li ion/Li–O_2 cells. *J. Phys. Chem. Lett.* **4,** 3607–3611 (2013).
13. Scrosati, B., Hassoun, J. & Sun, Y.-K. Lithium-ion batteries. A look into the future. *Energy Environ. Sci.* **4,** 3287–3295 (2011).
14. Sharon, D. *et al*. Lithium-oxygen electrochemistry in non-aqueous solutions. *Isr. J. Chem.* **55,** 508–520 (2015).
15. Johnson, L. *et al*. The role of LiO_2 solubility in O_2 reduction in aprotic solvents and its consequences for Li–O_2 batteries. *Nature Chem.* **6,** 1091–1099 (2014).
16. Aetukuri, N. B. *et al*. Solvating additives drive solution-mediated electrochemistry and enhance toroid growth in non-aqueous Li–O_2 batteries. *Nature Chem.* **7,** 50–56 (2015).
17. Luntz, A. C. *et al*. Tunneling and polaron charge transport through Li_2O_2 in Li–O_2 batteries. *J. Phys. Chem. Lett.* **4,** 3494–3499 (2013).
18. Hummelshoj, J. S., Luntz, A. C. & Norskov, J. K. Theoretical evidence for low kinetic overpotentials in Li–O_2 electrochemistry. *J. Chem. Phys.* **138,** 034703 (2013).
19. Laoire, C. O., Mukerjee, S., Abraham, K. M., Plichta, E. J. & Hendrickson, M. A. Influence of nonaqueous solvents on the electrochemistry of oxygen in the rechargeable lithium-air battery. *J. Phys. Chem. C* **114,** 9178–9186 (2010).
20. Schwenke, K. U., Metzger, M., Restle, T., Piana, M. & Gasteiger, H. A. The influence of water and protons on Li_2O_2 crystal growth in aprotic Li–O_2 cells. *J. Electrochem. Soc.* **162,** A573–A584 (2015).
21. Adams, B. D. *et al*. Current density dependence of peroxide formation in the Li–O_2 battery and its effect on charge. *Energy Environ. Sci.* **6,** 1772–1778 (2013).
22. Burke, C. M., Pande, V., Khetan, A., Viswanathan, V. & McCloskey, B. D. Enhancing electrochemical intermediate solvation through electrolyte anion selection to increase nonaqueous Li–O_2 battery capacity. *Proc. Natl Acad. Sci. USA* **112,** 9293–9298 (2015).
23. Aurbach, D. *et al*. *The Catalytic Behavior of Lithium Nitrate in Li–O_2 Batteries.* The 228th ECS Meeting, Phoenix, Arizona, 11–15 October (2015).
24. Gunasekara, I., Mukerjee, S., Plichta, E. J., Hendrickson, M. A. & Abraham, K. M. A study of the influence of lithium salt anions on oxygen reduction reactions in Li–air batteries. *J. Electrochem. Soc.* **162,** A1055–A1066 (2015).
25. Khetan, A., Luntz, A. & Viswanathan, V. Trade-offs in capacity and rechargeability in nonaqueous Li–O_2 batteries: solution-driven growth versus nucleophilic stability. *J. Phys. Chem. Lett.* **6,** 1254–1259 (2015).
26. Sharon, D. *et al*. Oxidation of dimethyl sulfoxide solutions by electrochemical reduction of oxygen. *J. Phys. Chem. Lett.* **4,** 3115–3119 (2013).
27. Lacey, M. J., Frith, J. T. & Owen, J. R. A redox shuttle to facilitate oxygen reduction in the lithium air battery. *Electrochem. Commun.* **26,** 74–76 (2013).
28. Yang, L., Frith, J. T., Garcia-Araez, N. & Owen, J. R. A new method to prevent degradation of lithium-oxygen batteries: reduction of superoxide by viologen. *Chem. Commun.* **51,** 1705–1708 (2015).
29. Sun, D. *et al*. A solution-phase bifunctional catalyst for lithium-oxygen batteries. *J. Am. Chem. Soc.* **136,** 8941–8946 (2014).
30. Matsuda, S., Hashimoto, K. & Nakanishi, S. Efficient Li_2O_2 formation via aprotic oxygen reduction reaction mediated by quinone derivatives. *J. Phys. Chem. C* **118,** 18397–18400 (2014).
31. Imanishi, N., Luntz, A. C. & Bruce, P. G. *The Lithium Air Battery: Fundamentals* (Springer, 2014).
32. Guin, P. S., Das, S. & Mandal, P. C. Electrochemical reduction of quinones in different media: a review. *Int. J. Electrochem.* **2011,** 1–22 (2011).
33. Saveant, J.-M. *Elements of Molecular and Biomolecular Electrochemistry: An Electrochemical Approach to Electron Transfer Chemistry* (John Wiley, 2006).
34. Hartmann, P. *et al*. A rechargeable room-temperature sodium superoxide (NaO_2) battery. *Nature Mater.* **12,** 228–232 (2013).
35. Ottakam Thotiyl, M. M., Freunberger, S. A., Peng, Z. & Bruce, P. G. The carbon electrode in nonaqueous Li–O_2 cells. *J. Am. Chem. Soc.* **135,** 494–500 (2013).
36. Chen, Y., Freunberger, S. A., Peng, Z., Fontaine, O. & Bruce, P. G. Charging a Li–O_2 battery using a redox mediator. *Nature Chem.* **5,** 489–494 (2013).
37. Lu, Y.-C. *et al*. The discharge rate capability of rechargeable Li–O_2 batteries. *Energy Environ. Sci.* **4,** 2999–3007 (2011).
38. McCloskey, B. D. *et al*. Combining accurate O_2 and Li_2O_2 assays to separate discharge and charge stability limitations in nonaqueous Li–O_2 batteries. *J. Phys. Chem. Lett.* **4,** 2989–2993 (2013).
39. Freunberger, S. A. *et al*. The lithium-oxygen battery with ether-based electrolytes. *Angew. Chem. Int. Ed.* **50,** 8609–8613 (2011).
40. Chen, Y., Freunberger, S. A., Peng, Z., Barde, F. & Bruce, P. G. Li–O_2 battery with a dimethylformamide electrolyte. *J. Am. Chem. Soc.* **134,** 7952–7957 (2012).
41. Adams, B. D. *et al*. Towards a stable organic electrolyte for the lithium oxygen battery. *Adv. Energy Mater.* **5,** 1400867 (2015).
42. Zhang, Z. *et al*. Increased stability toward oxygen reduction products for lithium-air batteries with oligoether-functionalized silane electrolytes. *J. Phys. Chem. C* **115,** 25535–25542 (2011).
43. Giordani, V. *et al*. *Freely Diffusing Oxygen Evolving Catalysts for Rechargeable Li–O_2 Batteries.* Abstract for 16th IMLB 2012 Jeju Korea S6–3 (2012).
44. Bergner, B. J., Schurmann, A., Peppler, K., Garsuch, A. & Janek, J. TEMPO: a mobile catalyst for rechargeable Li–O_2 batteries. *J. Am. Chem. Soc.* **136,** 15054–15064 (2014).
45. Lim, H. D. *et al*. Superior rechargeability and efficiency of lithium-oxygen batteries: hierarchical air electrode architecture combined with a soluble catalyst. *Angew. Chem. Int. Ed.* **53,** 3926–3931 (2014).
46. Trahan, M. J. *et al*. Cobalt phthalocyanine catalyzed lithium-air batteries. *J. Electrochem. Soc.* **160,** A1577–A1586 (2013).
47. Lee, M. *et al*. Redox cofactor from biological energy transduction as molecularly tunable energy-storage compound. *Angew. Chem. Int. Ed.* **52,** 8322–8328 (2013).
48. Hanyu, Y. & Honma, I. Rechargeable quasi-solid state lithium battery with organic crystalline cathode. *Sci. Rep.* **2,** 453 (2012).
49. Peover, M. E. & Davis, J. D. The influence of ion-association on the polarography of quinones in dimethylformamide. *J. Electroanal. Chem.* **6,** 46–53 (1963).

50. Koper, M. T. M. Thermodynamic theory of multi-electron transfer reactions: implications for electrocatalysis. *J. Electroanal. Chem.* **660,** 254–260 (2011).

Acknowledgements
P.G.B. is indebted to the EPSRC and the RCUK Energy programme including SUPERGEN for financial support.

Author contributions
X.G. and Y.C. designed experiments and analysed the data. X.G. performed electrochemical and characterization of discharge products. Y.C. performed the ultraviolet–visible spectroscopy experiments and analysed the data. P.G.B., X.G., Y.C. and L.J. interpreted the data. P.G.B. wrote the paper.

Additional information
Supplementary information is available in the online version of the paper. Reprints and permissions information is available online at www.nature.com/reprints. Correspondence and requests for materials should be addressed to P.G.B.

Competing financial interests
The authors declare no competing financial interests.

Methods

TEGDME was distilled under vacuum and DME was distilled under Ar. All solvents were further dried for several days over freshly activated molecular sieves (type 4 Å, Aldrich) before use. The final water content was <10 ppm (determined by Karl Fischer titration). Lithium bis(trifluoromethane)sulfonimide (LiTFSI, Aldrich) was dried at 70 °C under vacuum over several days. 3,5-di-*tert*-butyl-*o*-benzoquinone, 2,5-di-*tert*-butyl-1,4-benzoquinone (DBBQ) and thymoquinone were obtained from Aldrich. The prepared electrolyte solutions contain <10 ppm water content (determined by Karl Fischer titration). High-purity N5.5 O_2 (BOC) was used in all measurements. O_2 gas flow was further dried by an in-line moisture trap filled with activated 3 Å molecular sieves. All materials were stored in an Ar-filled glovebox.

Cyclic voltammetry was performed using a VMP3 electrochemical workstation (Biologic) and a multi-necked, air-tight glass cell within a glovebox. The measurements were carried out at room temperature and infrared correction was used. Polycrystalline Au discs (2-mm-diameter; BAS) were employed as the working electrodes. A platinum wire served as the counter electrode and a partially oxidized $LiFePO_4$ composite electrode behind a Vycor frit served as the reference electrode, as described previously[15].

Swagelok Li–O_2 cells were constructed as described previously[51]. Binder-free gas diffusion layers (GDLs, H2315, Quintech) served as the O_2 electrode. GDLs were heated under an Ar:H_2 (95:5 v/v) atmosphere at 900 °C for three hours. The porosity of the GDLs is ~80%, roughness factor (total surface area/areal area) is 90 and the Brunauer–Emmett–Teller surface area is below 1 $m^2\ g^{-1}$ (ref. 34). Three pieces of GDLs (4 mm × 4 mm) were stacked to form the cathode, giving a final roughness factor of 270 (3 × 90), a glass fibre filter (Waterman) was used as the separator and a partially oxidized $LiFePO_4$ electrode was used as the anode. The two-phase Li_xFePO_4 has a fixed potential of 3.45 V versus Li^+/Li. Two hundred microlitres of electrolyte solution was used, consisting of either TEGDME or DME containing 1 M LiTFSI with DBBQ as indicated in the main article. All cell components were dried at 90 °C under vacuum before use. Assembled cells were placed in glass tubes, which were filled with dried O_2 inside the glovebox. Cells were discharged inside an Ar-filled glovebox.

Characterizations of discharged electrodes. For post-cycling characterization, the cells were disassembled in a glovebox and the cathode and separators were rinsed with a small amount of TEGDME or DME; the resulting solutions were subjected to Karl Fischer titration to determine the water content after discharge. The electrodes were rinsed again with DME and dried before further characterization. The morphologies of discharge electrodes were observed by FE-SEM using a Zeiss-Merlin. PXRD was carried out with a Rigaku X-ray diffractometer in an air-sensitive holder. Fourier transform infrared spectra were measured with a Thermo IR spectrometer (Nicolet 6700) in a N_2-filled glovebox. Raman spectra were measured with a Renishaw inVia spectrometer (10 mW laser power at 785 nm) with an air-sensitive sample holder. For NMR analysis, 100 µl of electrolyte was extracted from the discharge electrodes and separators then diluted with 0.7 ml of $CDCl_3$; measurements were recorded on a Bruker spectrometer (400 MHz). A DEMS cell was constructed as described previously[40]. A GDL served as the working electrode and a partially oxidized $LiFePO_4$ composite electrode served as the anode. The electrolyte solution was 10 mM DBBQ in 1 M LiTFSI in TEGDME. A continuous 95% O_2/5% Ar gas flow was purged through the cell as a carrier gas at a flow rate of 0.3 ml min^{-1}.

The quantity of Li_2O_2 formed was determined by ultraviolet–visible spectrometry (Thermo Evolution 200) using an ultraviolet–visible titration method reported previously[20,52]. The unwashed discharged electrode and separators were added to a vial containing a known amount of water; Li_2O_2 reacts with water to produce H_2O_2 in solution. One millilitre of this solution was mixed with 2 ml of 2% $TiOSO_4$ dissolved in 1 M H_2SO_4 solution and a yellowish complex $[Ti(O_2)]^{2+}$ ($\lambda_{max} = 405$ nm) was formed. The ultraviolet–visible absorption spectrum of the solution was measured and compared with a calibration curve, which was obtained by measuring solutions with known amounts of commercial Li_2O_2 (Aldrich). The purity of commercial Li_2O_2 was determined by titration using $KMnO_4$ and this was taken into account when constructing the calibration curve.

References

51. Ottakam Thotiyl, M. M. *et al*. A stable cathode for the aprotic Li–O_2 battery. *Nature Mater.* **12,** 1050–1056 (2013).
52. Hartmann, P. *et al*. A comprehensive study on the cell chemistry of the sodium superoxide (NaO_2) battery. *Phys. Chem. Chem. Phys.* **15,** 11661–11672 (2013).

Erratum: Promoting solution phase discharge in Li–O_2 batteries containing weakly solvating electrolyte solutions

Xiangwen Gao, Yuhui Chen, Lee Johnson and Peter G. Bruce

Nature Materials http://dx.doi.org/10.1038/nmat4629 (2016); published online 25 April 2016; corrected online 16 June 2016.

In the version of the Article originally published, the first author's name in ref. 43 should have read 'Giordani, V.'. This has been corrected in all versions of the Article.